760644

The Unsteady Gas Exchange Characteristics of a Two-Cycle Engine

G. P. Blair and M. C. Ashe
Mechanical Engineering Dept., (Northern Ireland)

THE FLOW OF GAS through an engine has interested both scientists and engineers since the early development and usage of the self-propelled vehicle. However, while the progress of the steam and gas turbine could proceed logically with the application of steady state and flow thermodynamics and gas dynamics, not so the reciprocating internal combustion engine. In this engine the gas flow and combustion processes, having decidedly unsteady flow and state characteristics which defy simplified theoretical treatment, progress for the first half of this twentieth century was of an experimental nature and the gas flow theories proposed were of an empirical nature. In this context it is not surprising that the work and theory of Kadenacy (1)* on exhaust effects was taken up with enthusiasm and used for many years until Giffen (2) showed that in reality the 'Kadenacy effect' was due to the motion of large amplitude pressure waves. In some ways this merely served to add to the confusion for while it had been shown that the motion of gas in the exhaust (or inlet) system was controlled by these pressure waves, little was known of their propagation and reflection characteristics and even less about the algebraic or arithmetic techniques necessary for engineering calculations. It certainly was not a standard topic on the engineering undergraduate curriculum. Great progress in this theoretical area was made by De Haller (3) and Jenny (4) by their method of characteristics solutions. Theories about wave reflection, motions along typical engine ducting and from engine cylinders were examined and experimentally verified by the University of Birmingham team of Mucklow, Bannister, Wallace, Mitchell and Nassif and resulted in an excellent series of publications of which reference (5) is typical. While much was learned of unsteady gas flow in an engine the combined R and D efforts up to the mid-fifties merely illustrated the arithmetic complexities of attempting to utilize it for the purpose of practical engine design or

* Numbers in parentheses designate References at end of paper

ABSTRACT

The theoretical modelling of the scavenge process for a naturally aspirated two-cycle engine is described and employed in conjunction with an unsteady gas dynamic analysis of flow in the engine ducting. Programmed for a digital computer, the results of this theoretical study are shown in relation to a 250 cm^3 engine with values of predicted charging efficiency, scavenging efficiency, and delivery ratio given as a function of engine speed. These are compared with measured values of scavenging efficiency and the usual performance characteristics of power, mean effective pressure, delivery ratio, and specific fuel consumption. Also compared are the measured and predicted pressure diagrams taken in the cylinder, the crankcase, and the exhaust and inlet ducts. The design of a somewhat unique cylinder gas sampling valve of the mechanical type is described and its usage discussed both theoretically and practically.

development. At this point in engineering history the digital computer made its debut and Benson et al (6) showed that it could be used to solve the complex arithmetic associated with the calculation of unsteady gas motion in engine ducts.

At The Queen's University of Belfast efforts were made to apply this theoretical approach to the naturally aspirated two (and four) stroke cycle engine. The approach used was to check out each type of engine duct in turn by simulation of the unsteady flow with cold air and show that the theory was applicable to, and accurate in, a simplified system before converting it for use for firing engine calculations. Blair and Johnston (7) investigated exhaust systems, Blair and Arbuckle (8) analysed induction systems before Blair and Cahoon (9) combined the two previous works into a study of unsteady flow through a two-stroke cycle engine of the naturally aspirated type. In this last work the gas in the engine, be it exhaust or induction, is treated theoretically as if it were air only, abbeit at quite different state conditons, and although this allows accurate prediction of open cycle cylinder, and all exhaust, transfer, and induction pressures and mass flow rates it precludes the deduction of, for example, scavenging efficiency. Thus while volumetric efficiency could be calculated and compared with experimental values, as could exhaust, induction, transfer, and cylinder pressure-time histories, there was no possibility of predicting scavenging, trapping, and charging efficiencies with an air-only theoretical model. Nevertheless, the work showed that such a model was possible and the theoretical predictions from it correlated well with experimental measurements.

The next phase of this research program was to provide a suitable theoretical model to differentiate between exhaust gas and the fresh charge during the open cycle period with the motions of each monitored in order that at exhaust closure, or trapping, the total mass of trapped charge is predicted, as is its purity. This paper sets out such a theoretical model for the scavenging part of the open cycle and shows its application to the theoretical study of a 250 cm^3 Husqvarna engine. In the experimental section, apart from the normal performance measurements of power, torque, specific fuel consumption, etc., the scavenging efficiency of the engine is measured by the use of a gas sampling valve of the mechanical type. It is of somewhat unique design and has the desirable attribute of allowing some 30-40% of the trapped charge to be removed from the cylinder for chemical analysis and subsequent evaluation of scavenging efficiency. The scavenging efficiencies so measured are then compared to those calculated by the theoretical model; comparisons of measured and calculated cylinder, exhaust, intake, and crankcase pressure-time histories are also made and improved correlation is shown to exist over the air-only theoretical model of Blair and Cahoon (9). Finally, the computed charging efficiency is shown to have good correlation with the engine torque (or bmep).

EXPERIMENTAL APPARATUS

The engine used in the experimental program is the 250 cm^3 Husqvarna moto-cross unit, model MI250 and is a single cylinder, two-cycle, naturally aspirated, spark-ignition, loop-scavenged design with piston-controlled induction. The significant engine dimensions are shown in the table, Fig. 1. The ignition

Husqvarna single cylinder, loop-scavenged two-stroke engine	
Model	MI 250
Bore	69.5 mm
Stroke	64.5 mm
Connecting rod centres	120.0 mm
Trapped compression ratio	7.0:1
Crankcase compression ratio	1.5:1
Exhaust port opens	90° atdc
Transfer ports open	120° atdc
Inlet port opens	80° btdc
Number of exhaust ports	1
Exhaust port width	42.0 mm
Number of transfer ports	5
Effective transfer port width	77.0 mm
Number of Inlet Ports	2
Total effective inlet port width	42.0 mm
Maximum inlet port height	28.0 mm
Carburettor diameter	36.0 mm
Length of inlet tract	185.0 mm
Length of transfer passages	76.0 mm

Fig. 1 - Significant engine measurements

system used is the Motoplat electronic (breakerless) unit which has the advantage of consistent precision spark timing. Many exhaust ducts were used during the experimental program but for simplified contrast the results of two, namely MK1 (standard) and MK4, are described in this paper. Their significant dimensions are shown in Fig. 2. The engine drives a Heenan and Froude DPXO water dynamometer, and other performance parameters measured are air and fuel consumption. Air consumption is measured by the air box and orifice (BS1042, 1966) method and fuel consumption rate is determined by timing the usage of a 100 cm^3 gasoline quantity. The results are corrected for atmospheric conditions by SAE standard engine test procedures for power, brake mean effective pressure, brake specific fuel consumption, air/fuel ratio, and delivery ratio. A photograph of the engine and test-bed is shown in Fig. 3.

To study the unsteady gas flow through

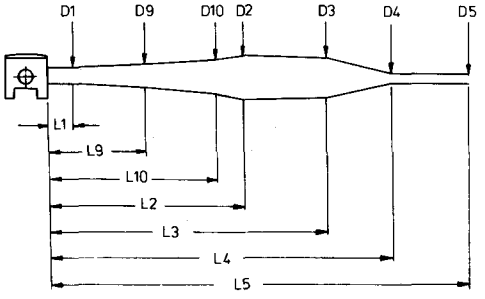

Dimension	MK.1.	MK.4
L1(mm)	455	75
L9	480	460
L10	610	685
L2	685	735
L3	915	940
L4	1120	1220
L5	1220	1450
D1(mm)	49.0	49.0
D9	62.5	66.0
D10	74.5	96.0
D2	95.0	110.0
D3	95.0	100.0
D4	38.0	28.5
D5	38.0	28.5

Fig. 2 - Exhaust system dimensions

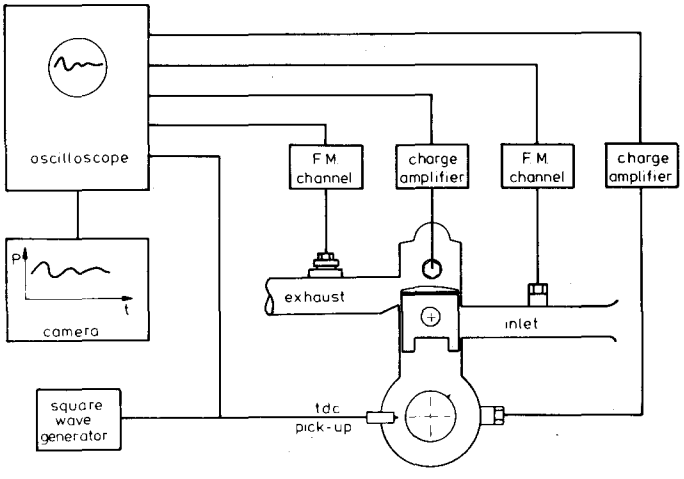

Fig. 4 - Layout of pressure measurement apparatus

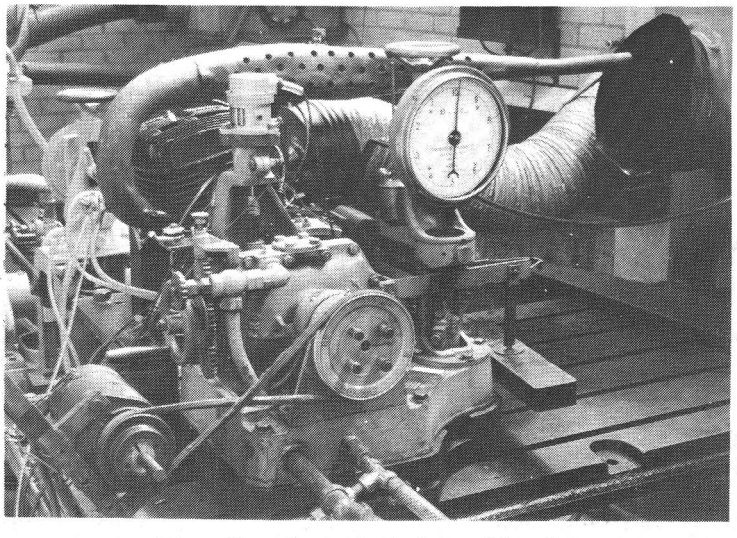

Fig. 3 - Test-bed installation

the engine, measurements of the static pressure behaviour are taken at strategic points in the engine system. Two basic types of transducer are used, the final choice being dictated by the local environment and requirements at each position. These positions are (i) inlet tract (ii) crankcase (iii) cylinder, but open cycleand (iv) exhaust duct. A general arrangement of the layout and recording media is shown in Fig. 4. Capacitance transducers, Southern Instruments type G201 and G202 (10 and 50 lb/in^2), are used in the inlet and exhaust systems and are located at 2.25 and 6 in from the piston face respectively. These are employed for their excellent thermal drift (lack of) characteristics in these locations. Piezo-electric transducers, Vibrometer type 12QP250 cv are used to measure crankcase and open-cycle cylinder pressures. The cylinder transducer, which is recording over the range -3 to + 80 lb/in^2 in typical operation has significant thermal drift problems if operated in the static mode. However, this problem is overcome by utilizing it in the dynamic mode and calibrating its reference level dynamically by connecting it during a non-significant crank-angle period to the crankcase pressure. This was done by drilling a hole in the piston at the appropriate place, see Fig. 5.

All pressure traces, and associated top-dead-centre piston position marker with a 1 kHz square wave timing trace are displayed on an eight channel Tektronix type 565 oscilloscope and photographed by a Southern

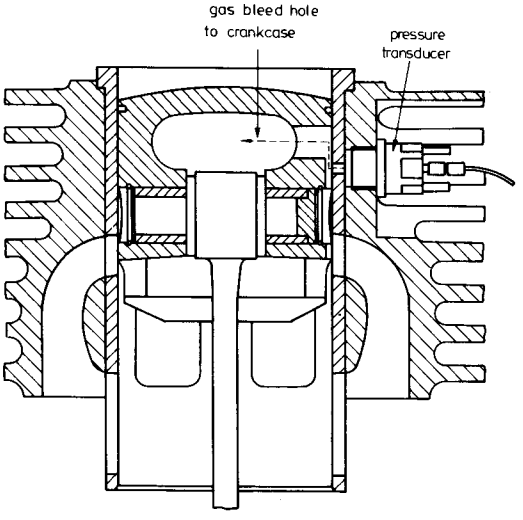

Fig. 5 - Gas connection of cylinder transducer to crankcase pressure

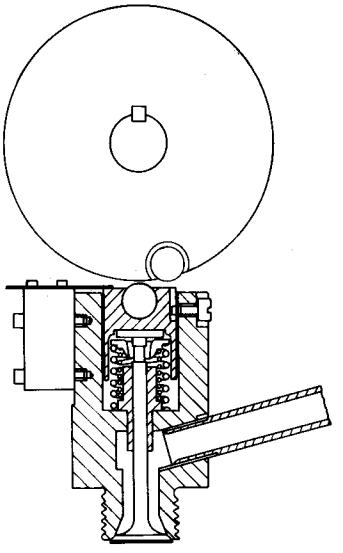

Fig. 6 - Gas sampling valve

Instruments type M906 drum camera loaded with Ilford NS6 120 mm wide x 1400 mm long paper. Drum speed is adjusted so as to record at least two engine cycles on this film. All traces are reduced to pressure (atm)/crank-angle plots by a D-Mac trace-follower, the paper tape output from which is inputed to the University's ICL 1906S computer and are drawn on a Calcomp graph plotter.

As one of the main objects of the experimental program is to measure accurately scavenging efficiency, a sampling valve design was necessary to extract compression gas samples after exhaust closure (trapping) and before firing. The objective in any Schnurle scavenged engine is to stratify, or separate the incoming fresh charge from the exhaust products. Thus it seems desirable to have a sampling valve which will extract as much of the trapped charge as possible in order that the scavenging efficiency, or charge purity, of this 'stratified' mixture can be accurately assessed. As electromagnetic sampling valves would typically extract some 6% of the trapped charge (11) in the Husqvarna 250 at 5000 rev/min, and perhaps 3% at 8000 rev/min, then some other means of sampling seemed desirable, if not essential, and a mechanically operated unit was designed as a simple alternative (12). A sectioned sketch of the device used is shown in Fig. 6 and a photograph of it mounted on the engine appears in Fig. 7.

The objective is to extract as much as possible of the contents of the cylinder once in every eleven engine cycles at an accurate and predetermined phase position. It consists essentially of a poppet valve located in a steel body which is screwed into a specially constructed cylinder head, the profile of which and its compression ratio, are identical to that used for the previous performance and pressure-time diagram experiments.

The valve, valve springs, collets, and retaining ring are all stock items from a 50 cm^3 Honda four-cycle motor cycle engine. Immediately above the valve is a hardened steel shim and an aluminium cam follower bearing a 0.438 in diameter hardened steel roller. Also mounted in the cylinder head are two self-aligning bearing brackets. These carry a 0.75 in diameter steel shaft on which is keyed a camwheel see Figs. 6 and 7. This camwheel carries another 0.438 in diameter roller. Drive to the camwheel is achieved by an 8mm Renolds chain from a 9 tooth sprocket on the crankshaft to a 99 toothed wheel on the "overhead camshaft", that being essentially the mechanism.

With the engine running the camshaft rotates at 1/11 th of crankshaft speed so that on each 11 th cycle the two hardened steel rollers make contact causing the valve to open. In order to compensate somewhat for the lack of 'ramp angle, etc.', on the 'cam profile', and reduce the forces generated at the instant of contact, the camwheel roller is encased in a nylon insert. After the sampled cycle the engine runs normally for a further 10 cycles allowing a stable firing mode of operation before the next sample is taken.

A diagrammatic sketch of the gas sampling layout is shown in Fig. 8. To record the opening and closing of the valve a simple make/break contact system is attached to the valve body, see Fig. 6. A spring steel pointer makes contact with the cam follower and as the valve opens contact is lost, breaking the electrical circuit to the oscilloscope shown in Fig. 8. As a means of preventing ignition when extracting compression gas samples a further set of contact-breaker points is incorporated in the system. These, mounted on a bracket attached to the cylinder

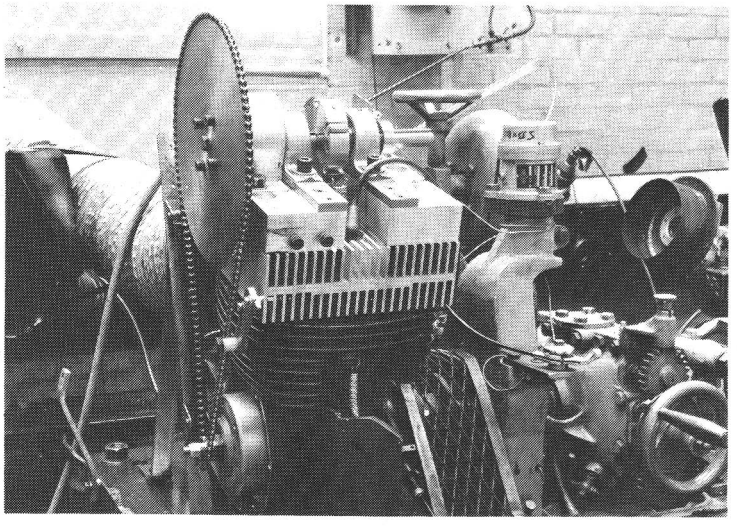

Fig. 7 - Gas sampling and cylinder head installation

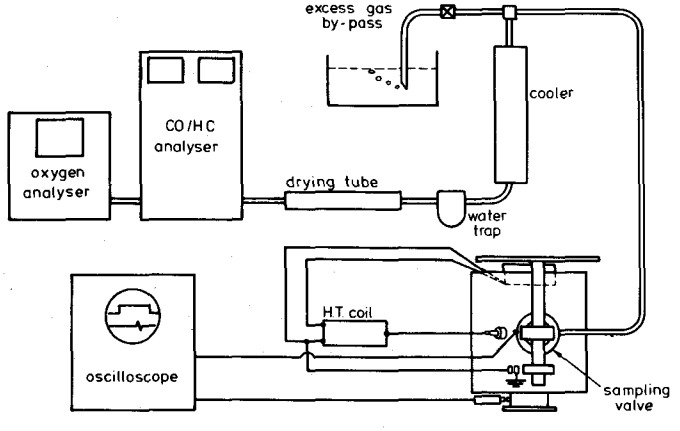

Fig. 8 - Layout of gas sampling apparatus

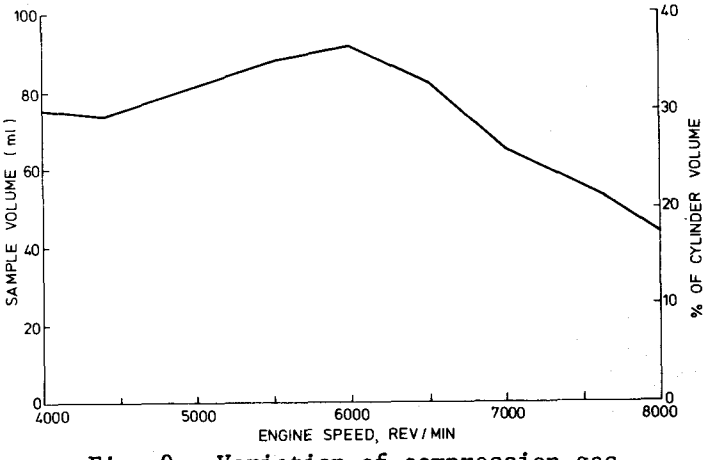

Fig. 9 - Variation of compression gas sample volume with engine speed

head, are operated by a separate cam on the overhead camshaft. Normally the points are held in the open position but during the sampled cycle a flat on the cam allows the points to close, earthing the primary ignition circuit, thus preventing an ignition spark.

As one of the objects of the design is to obtain large samples, Fig. 9 is of interest. This shows both the sample volume, and its proportion of cylinder volume, against engine speed. Bearing in mind that this is a 250 cm^3 swept volume engine, Fig. 9 illustrates that a minimum of 18% (and a maximum of 35%) is being extracted for sampling purposes.

The gas extracted from the engine, either expansion or compression gas, is passed through a cooler, a water trap, a drying tube, and thence to a CO/HC analyser and finally an oxygen analyser. The operation is on-line analysis of a dried gas sample with all but the lightest hydrocarbons removed.

When taking compression gas samples the cooler is filled with dry ice and acetone, achieving temperatures as low as -60°C and all but the lightest hydrocarbons will be condensed. When sampling expansion gas cold water is circulated through the cooler and the water vapour is condensed and caught in the following water trap. A drying tube filled with magnesuim perchlorate removes any remaining moisture.

The gas analyser for carbon monoxide and hydrocarbons (CO/HC) is a Horiba unit type Mexa 300. This is a double-beam unit of the non-dispersive infra-red type and gives a direct read-out of the concentration by volume of the gases simultaneously on two separate meters. The analyser used for oxygen determination is the Taylor-Servomex Type OA250, and is of the paramagnetic type.

All gas sampling tests and pressure-time diagram recordings are recorded, at any particular engine speed, at the identical air/fuel ratio as determined for the performance characteristics, in other words as if all operations were being performed

simultaneously. Due to the experimental complexities, performance/speed characteristics were first determined and then the pressure-time diagram recording and gas sampling performed as two further and separate experiments.

THEORETICAL EVALUATION

The theoretical approach used by Blair and Cahoon (9) applies here, but with the significant improvement of tracing separately the movements and state conditions of exhaust products and fresh charge and defining a model for the gas exchange (or scavenge) process in the cylinder during the open cycle of operation. Therefore there is no point in repeating the unsteady gas dynamic theory of Blair and Cahoon (9), and this section concentrates on the theoretical model for the gas exchange process.

PREDICTED GAS PURITY IN THE ENGINE CYLINDER, AND IN THE TRANSFER AND EXHAUST TRACTS The purity of gas within a particular boundary or control volume is defined as the ratio of the mass of fresh charge present to the total mass present. In order to predict the gas purity in the cylinder or at any point in the transfer or exhaust systems, it is necessary to trace the flow of gas through the engine system. This is best achieved by dividing the transfer and exhaust pipes into a number of control volumes. It is convenient to terminate these control volumes with the equi-spaced mesh points already used in the unsteady gas flow analysis, as described by Blair and Cahoon (9).

Since engine scavenging behaviour normally lies somewhere between perfect scavenging (i.e. displacement without mixing) and perfect mixing, an analysis is derived which considers both possibilities in the cylinder.

The following assumptions are made in the analysis:

1. Each control volume is contained between adjacent mesh points and is designated as in Fig. 10.
2. The cylinder control volume is bounded by the transfer and exhaust ports, cylinder head, liner and piston.
3. Perfect mixing takes place in all the control volumes in the transfer and exhaust tracts.
4. Either perfect scavenging or perfect mixing takes place within the cylinder.
5. Complete combustion takes place in the cylinder (i.e. there is no fresh charge present at exhaust port opening).
6. The gas in the crankcase and inlet pipe consists entirely of fresh charge (i.e. there is negligible flow of burnt charge from transfer to crankcase).

Gas Purity in the Exhaust and Transfer Tracts For clarity of presentation the computer indexing system is retained and the

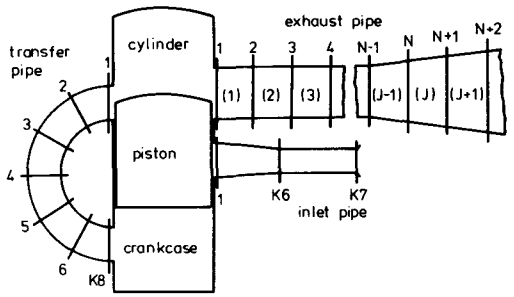

Fig. 10 - Layout of control volumes for 'purity' calculations

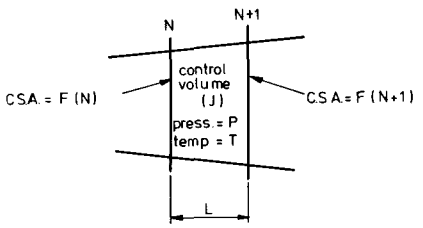

Fig. 11 - Typical control volume

letters N and J are used to identify mesh points and control volumes respectively. Therefore F(N) refers to the cross-sectional area of the pipe at the Nth mesh point, and F(N+1) is the area at the next mesh point. The subscripts 1 and 2 indicate conditions at the beginning and end of a computer cycle. Thus M1(J) denotes the mass in the Jth control volume at the start of a computer cycle and M2(J) denotes the mass at the end of that cycle.

With a knowledge of the geometry of the tracts the initial mass of transfer and exhaust control volumes can be obtained from the equation of state,

$$PV = MRT \qquad (1)$$

Referring to Fig. 12 and rearranging equation (1) gives an expression for M1(J)

$$M1(J) = \frac{F(N) + F(N+1)}{2} . L . \frac{P}{R.T} \qquad (2)$$

The instantaneous mass flow rate across each mesh point is given by:

$$\dot{m} = \rho . F . u \qquad (3)$$

which on substituting for ρ from the isentropic relationship

$$\left(\frac{a}{a_o}\right)^{\frac{2\gamma}{\gamma-1}} = \left(\frac{\rho}{\rho_o}\right)^{\gamma}$$

and for u from the non-dimensional velocity

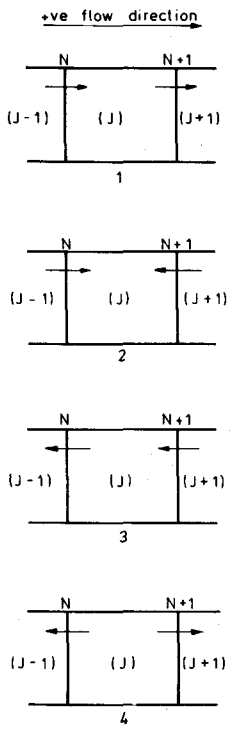

Fig. 12 - Possible flow combinations

term

$$U = \frac{u}{a_o}$$

becomes

$$\dot{m} = \rho_o \left(\frac{a}{a_o}\right)^{\frac{2}{\gamma-1}} . F . U . a_o \qquad (4)$$

Using the pseudo-Riemann variable forms of $\frac{a}{a_o}$ and U, equation 4 can be rewritten as

$$\dot{m} = \rho_o \left(\frac{\lambda + \beta}{2}\right)^{\frac{2}{\gamma-1}} . F . \left(\frac{\lambda - \beta}{\gamma - 1}\right) . a_o$$

$$= \frac{1}{\gamma - 1} \cdot a_o . F . (\lambda - \beta) . \left(\frac{\lambda + \beta}{2}\right)^{\frac{2}{\gamma-1}} \rho_o \qquad (5)$$

For a small time increment ΔZ, the transfer of mass across the Nth mesh is given by

$$M(N) = \frac{1}{\gamma - 1} \cdot a_o . F(N) . [\lambda(J) - \beta(J)]$$

$$\cdot \left[\frac{\lambda(J) + \beta(J)}{2}\right]^{\frac{2}{\gamma-1}} \rho_o \Delta Z \qquad (6)$$

The terms a_o and ρ_o denote reference conditions in the pipes concerned and are changed to the appropriate values depending on whether it is the transfer or exhaust pipe which is under consideration.

Knowing the mass and purity within each control volume and recording the magnitude and purity of the flow into and out of each, the new mass and purity can be calculated. The new mass, M2(J), within the Jth control volume can be expressed as follows:

$$M2(J) = M1(J) + \Delta M(N) - \Delta M(N + 1) \qquad (7)$$

There is, however, more than one expression for the new purity of the gas within the control volume. Since there are two flow directions for both inflow and outflow, four equations are necessary to take all possible flow conditions into account. The modes of flow which can prevail are shown in Fig. 12. The relevant expressions for the new purity in the control volume are given below.

Positive inflow, positive outflow The gas flowing into the Jth control volume is coming from the (J - 1)th control volume and is, therefore, of purity $\phi 1(J - 1)$. The gas flowing out of the Jth control volume is M1(J) and is of purity $\phi 1(J)$.

Therefore the mass of pure gas in the Jth control volume at the end of a time increment is

$$M1(J).\phi 1(J) + \Delta M(N).\phi 1(J - 1) - \Delta M(N + 1).\phi(J)$$

initial value flowing in flowing out

The new purity within the control volume is given by

$$\phi 2(J) = \frac{M1(J).\phi 1(J) + \Delta M(N).\phi(J-1) - \Delta M(N+1).\phi 1(J)}{M2(J)} \qquad (8)$$

Similar reasoning follows for the other three modes of flow.

Gas Purity Within the Cylinder - Scavenging Efficiency The cylinder is regarded as a control volume with flow through the exhaust and transfer ports. The magnitude of this flow, and its direction, can be calculated from Eq. 6 after replacing F(N) by the area of port opening. Once more, four possible flow conditions through the ports can exist as well as the alternatives of perfect scavenging or perfect mixing in the cylinder. The sign convention used is:

exhaust flow out of cylinder: positive
trasfer flow into cylinder: positive

Using this sign convention the new cylinder mass CM2, after a time increment ΔZ can be expressed as

$$CM2 = CM1 + \Delta MTR - \Delta MEX \qquad (9)$$

Consider the 'normal' flow pattern of positive transfer and positive exhaust flow for both perfect scavenging and perfect mixing within the cylinder

Perfect Mixing Under these conditions gas of purity $TR\phi(1)$ is flowing into the cylinder from the first control volume in the transfer pipe. The gas flowing out of the cylinder is of purity $C\phi1$. Therefore the new cylinder purity at the end of a time increment is given by

$$C\phi2 = \frac{CM1.C\phi1 + \Delta MTR.TR\phi(1) - \Delta MEX.C\phi1}{CM2} \quad (10)$$

Perfect Scavenging Again, gas of purity TR (1) flows into the cylinder from the transfer duct. However under conditions of perfect scavenging. This gas remains separate from the burnt charge in the cylinder, so that the purity of gas flowing into the exhaust tract is of purity zero. Therefore, the new cylinder purity is given by

$$C\phi2 = \frac{CM1.C\phi1 + \Delta MTR.TR\phi(1) - \Delta MEX(0.0)}{CM2}$$

$$= \frac{CM1.C\phi1 + \Delta MTR.TR\phi(1)}{CM2} \quad (11)$$

The case of negative exhaust flow, i.e. flow from exhaust into cylinder, is not considered in this section since it can hardly be regarded as fitting into the category of perfect scavenging. Such a flow possibility occurs with a tuned exhaust system near the end of the transfer period and is dealt with as a 'perfect mixing' process.

The other flow possibilities are dealt with in a similar and logical manner and are not included here for the sake of brevity.

The model used for scavenging within the cylinder is a two-part one, and it is considered that the scavenge process commences at transfer port opening and proceeds for a pre-determined number of crankshaft degrees of engine notation, called SCAVDEG, as a 'perfect scavenging' process, and thereafter until exhaust closure as a 'perfect mixing' process. The first part of the model does not preclude the quite normal possibility of reverse flow from cylinder to transfer at transfer port opening in which case when crankcase pressure exceeds cylinder pressure and flow reverses to normality the charge entering the cylinder is still perfectly 'scavenged' but will be mainly exhaust gas of purity $TR\phi(1)$.

With the preceding theory in the form of a computer subroutine called 'Pure' inserted into the "Throughflow" program (9) it is possible to calculate the gas purity in the cylinder at any juncture. It is at trapping that it has major significance for scavenging efficiency is defined as

Scavenging efficiency, η_s =

$$\frac{\text{mass of fresh charge in cylinder at trapping}}{\text{total mass in cylinder at trapping}} \quad (12)$$

Knowing this, the charging efficiency defines the effectiveness of filling the cylinder with fresh charge, thus

Charging efficiency, η_c =

$$\frac{\text{mass of fresh charge in cylinder at trapping}}{\text{mass related to stroke volume of cylinder at STP}} \quad (13)$$

This latter value is related to torque, or bmep, for at equal conditions of compression ratio, ignition timing, etc., a higher value of charging efficiency must result in greater torque at the identical engine speed.

Two further efficiencies can be defined:

Trapping efficiency, η_T =

$$\frac{\text{mass of fresh charge in cylinder at trapping}}{\text{mass of fresh charge supplied per cycle}} \quad (14)$$

Delivery Ratio, DR =

$$\frac{\text{mass of fresh charge supplied per cycle}}{\text{mass related to stroke volume of cylinder at STP}} \quad (15)$$

It is obvious that

$$\eta_c = DR.\eta_T \quad (16)$$

SAMPLED GAS COMPOSITION AND SCAVENGING EFFICIENCY In order to measure scavenging efficiency it is necessary to establish the relative proportions of each of the components which make up the cylinder contents. Ideally this is done by extracting a sample of compression gas and analysing it for all of the components present. Practically this raises problems for some compounds such as water and many hydrocarbons are either very difficult or impossible to measure mass levels accurately. In any case during the course of sample collection an inevitable temperature change occurs resulting in condensation of some of the constituents and an apparent change of sample composition. Thus the sample is prepared by removing water and all but the lightest hydrocarbons.

The experimental apparatus records the volume concentration of oxygen, carbon monoxide, and hydrocarbons (hexane equivalent). But both compression and expansion gas samples can be taken. An analysis had to be derived therefore which would relate scavenging efficiency to the concentration of these three components in both samples.

The basic combustion process will proceed as follows:

fresh charge + exhaust gas fraction
→ expansion gas

For 1 mole of hydrocarbon fuel CH_y this process is represented by the chemical equation

$$CH_y + (S1)O_2 + S2(N_2) + B.[(X1)CO + (X2)CO_2 + (X3)H_2 + (X4)N_2 + (X5)O_2 + (X6)C_pH_q + (X7)H_2O] = (X1)CO + (X2)CO_2 + (X3)H_2 + (X4)N_2 + (X5)O_2 + (X6)C_pH_q + (X7)H_2O \quad (17)$$

For a known air/fuel ratio, AF

$$\text{then} \quad AF = \frac{32(S1) + 28(S2)}{(12 + y)} \quad (18)$$

$$\text{and} \quad S2 = \frac{79}{21} S1 \quad (19)$$

Combining (18) and (19)

$$S1 = \frac{(12 + y)AF}{137.33} \quad (20)$$

A carbon balance across Eq. 17 gives, where W = 1 - B

$$1 = W.X1 + W.X2 + W.p.X6 \quad (21)$$

a hydrogen balance produces

$$y = 2W.X3 + q.W.X6 + 2W.X7 \quad (22)$$

A nitrogen balance results in

$$S2 = W.S4 \quad (23)$$

an oxygen balance gives

$$2S1 = W.S1 + 2W.X2 + 2W.X5 + W.X7 \quad (24)$$

Fig. 13 and 14 illustrate diagrammatically the molal effects of sample preparation of compression and expansion gas respectively. Referring to Fig. 13, the volume fraction of carbon monoxide in the prepared compression gas, VFCOCG, is

$$VFCOCG = \frac{B.X1}{S1+S2+B(X1+X2+X3+X4+X5)} \quad (25)$$

and the volume fraction of oxygen, VFO2CG, is

$$VFO2CG = \frac{S1 + B.X5}{S1+S2+B(X1+X2+X3+X4+X5)} \quad (26)$$

Referring to the dried sample of expansion gas in Fig. 14 the volume fraction of carbon monoxide, VFCOEG, is

$$VFCOEG = \frac{X1}{X1+X2+X3+X4+X5+X6} \quad (27)$$

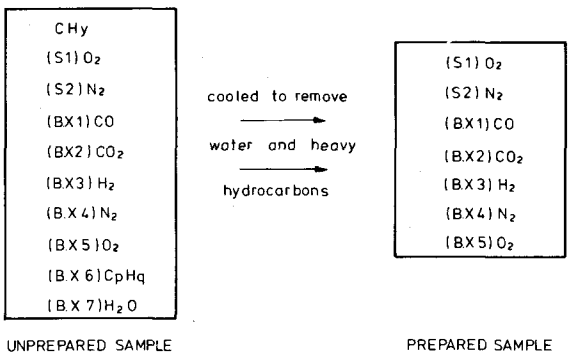

Fig. 13 - Compression gas sample

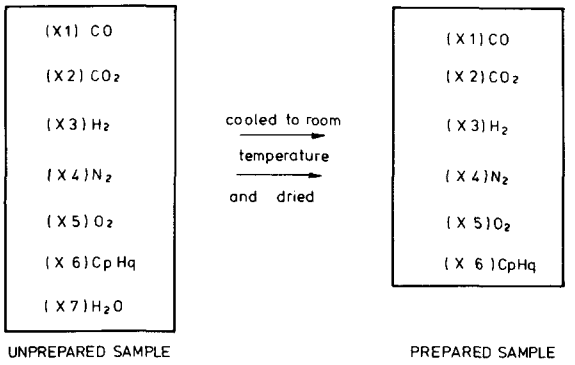

Fig. 14 - Expansion gas sample

and for hydrocarbons, VFHCEG, it is

$$VFHCEG = \frac{X6}{X1+X2+X3+X4+X5+X6} \quad (28)$$

and for oxygen, VFO2EG, it is,

$$VFO2EG = \frac{X5}{X1+X2+X3+X4+X5+X6} \quad (29)$$

These volume fractions are, of course, the actual measurements taken. Eqs. 21 to 29 represent a system of nine equations with eight unknowns, B, X1 .... X7, and the solution is best achieved by numerical methods and is so done at Q.U.B. using a computer subroutine written by the Nottingham Algorithms Group (N.A.G.), F04 AMF, which gives an accurate least squares solution of an overdetermined set of linear equations. When this has been effected and values of B, X1 .... X7 found, then referring to the unprepared compression gas sample in Fig. 13 the scavenging efficiency becomes determined.

Scavenging efficiency, η_s,

$$= \{12 + y + 32.S1 + 28.S2\}/\{12 + y + 32.S1 + 28.S2 + B[28.X1 + 44.X2 + 2.X3 + 28.X4$$

$+ 32.X5 + 12.p.X6 + q.X6 + 18.X7]\}$

The molal values p and q are set to 6 and 14 respectively for hydrocarbon concentrations are measured as hexane equivalent. The value y is set at 1.85 from information given for the gasoline/oil mixture by the supplying oil company.

EXPERIMENTAL AND THEORETICAL RESULTS AND DISCUSSION

PERFORMANCE CHARACTERISTICS The performance characteristics of the 250cm^3 Husqvarna engine with the MK1 and MK4 exhaust systems are shown in tabular form in Figs. 15 and 16 and in graphical layout in Figs. 17 and 18. The air/fuel ratios have been

MK1 ENGINE TEST DATA

Speed (rpm)	bhp	bmep	delivery ratio	bsfc	Air/fuel ratio
4000	9.86	65.3	0.672	0.978	11.08
4400	11.38	68.5	0.594	0.811	11.25
5000	15.80	83.7	0.857	0.995	10.82
5500	20.87	100.5	0.930	0.855	11.40
6000	26.28	116.0	0.932	0.754	11.22
6250	27.40	116.1	0.928	0.747	11.25
6500	28.58	116.5	0.927	0.763	10.98
7000	28.22	106.8	0.889	0.796	11.00
7600	26.23	91.4	0.820	0.847	11.15
8000	25.45	84.3	0.752	0.854	10.98

Fig. 15 - MK1 engine test data

MK4 ENGINE TEST DATA

Speed (rpm)	bhp	bmep	delivery ratio	bsfc	Air/fuel ratio
4000	9.78	64.5	0.621	0.911	11.06
5200	22.24	113.2	1.054	0.920	10.65
5500	25.39	122.2	1.059	0.814	11.20
6000	27.43	121.1	0.998	0.766	11.31
6500	26.54	108.1	0.993	0.864	11.17
7000	29.68	112.3	0.959	0.789	11.39
7500	22.84	80.6	0.888	1.001	11.56
8000	23.49	77.8	0.772	0.909	11.49

Fig. 16 - MK4 engine test data

kept level at about 11:1 and are also at an optimum, yet the two exhaust systems produce disparate behaviour.

Peak torque for the MK1 system is at 6500 rev/min while for the MK4 exhaust it is at 5500 rev/min. The latter also produces the higher delivery ratio values. It will also be observed that the mean effective pressure values are high, in excess of 115 lb/in^2 and the specific power output is about 120 bhp/litre, typical for this type of moto-cross engine, plus a broad torque band of some 3000 rev/min is maintained for both exhaust systems.

PRESSURE-TIME DIAGRAMS The pressure-crankangle diagrams for the engine with both exhaust systems are presented in the following manner and it should be noted that in all cases the full line represents the experimental measurement and the dashed line the theoretical prediction from the 'Throughflow' computer program with the 'Pure' subroutine added. Also included in this theoretical program is an improved knowledge of discharge coefficients for all ports, for all flow directions, for varying piston positions and gas pressure ratios. This has not been included in this publication for it represents a totally separate experimental series and theoretical discussion; it should be the subject of an SAE paper at some later date.

The crankcase and inlet pressure diagrams are plotted separately on the same figure; similarly open cycle cylinder and exhaust pressure diagrams are plotted together on a single figure. The y axis, or pressure scale is P/P_o, or atm. The x-axis is a crankangle scale from top-dead-centre (TDC) to top-dead-centre while appropriate vertical lines denote inlet opening and closing (IO and IC), transfer openging and closing (TO and TC), and exhaust opening and closing (EO and EC), and bottom-dead-centre (BDC). For the MK1 exhaust system, crankcase and inlet diagrams appear in Figs. 19-24 for engine speeds at 4000, 5000, 6000, 6500, 7000 and 8000 rev/min and open cycle cylinder and exhaust diagrams at the same engine speeds in Figs. 25-30. For the MK4 exhaust system, crankcase and inlet diagrams appear in Figs. 31-36 for engine speeds at 4000, 5200, 5500, 6000, 7000, and 8000 rev/min an open cycle cylinder and exhaust diagrams at the same engine speeds in Figs. 37-42.

It will be observed that the correlation between measured and calculated pressure-crankangle diagrams is good at all speeds; indeed it has been improved by comparison with the earlier paper by Blair and Cahoon (9).

SCAVENGING EFFICIENCY The measured scavenging efficiencies for the MK1 and the MK4 exhaust systems attached to the engine are shown in Figs. 43 and 44. The full line denotes the measured values while the dashed line shows the theoretical results assuming a perfect mixing model only, i.e. SCAVDEG = 0. It will be observed that the measured scavenging efficiencies are high but are consistent with Asunuma (11), above 90% and virtually constant in the 'power band' of the engine. It can also be seen that a 'perfect mixing' model describes fairly

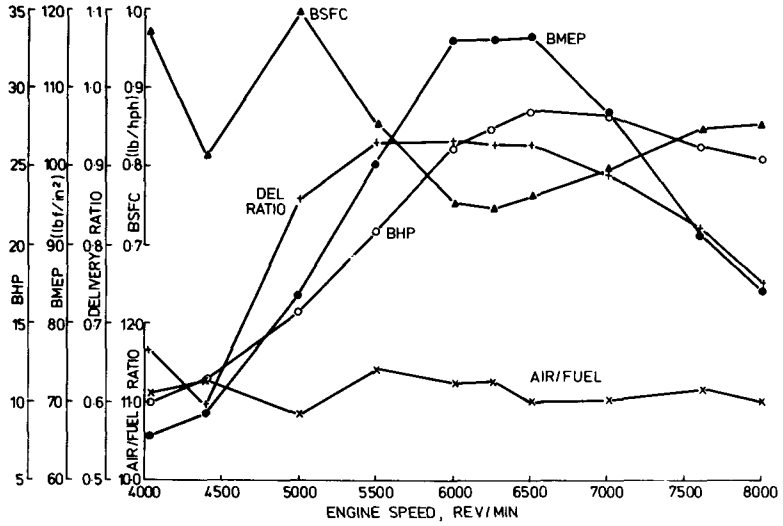

Fig. 17 - Performance characteristics of MK1 enigne

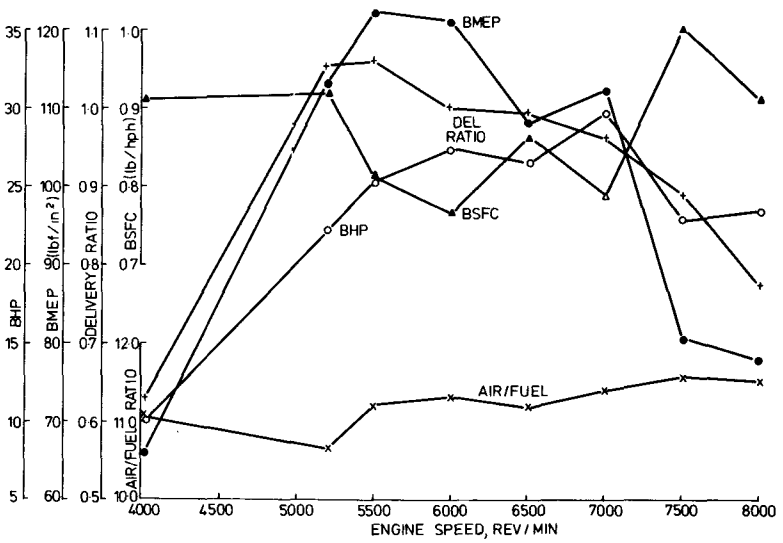

Fig. 18 - Performance characteristics of MK4 engine

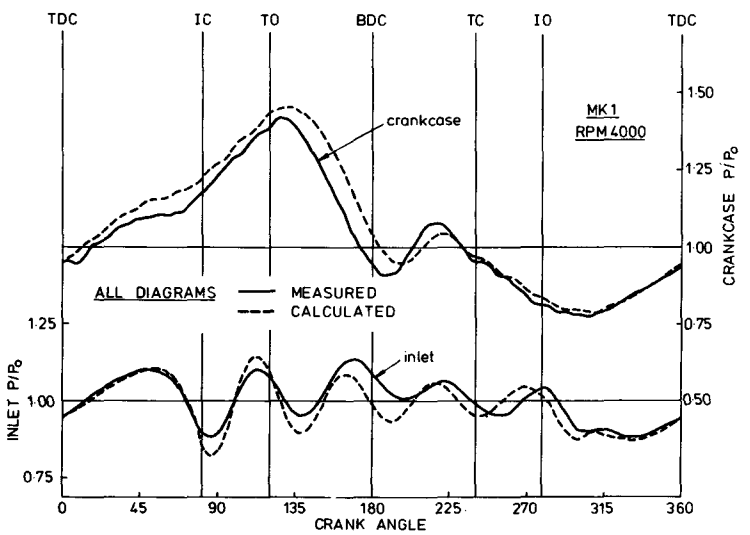

Fig. 19 - Crankcase and inlet pressures for MK1 at 4000 rpm

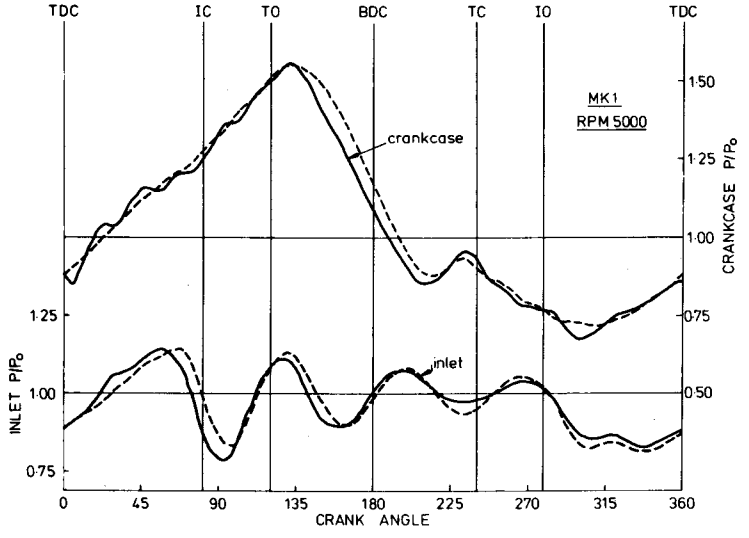

Fig. 20 - Crankcase and inlet pressures for MK1 at 5000 rpm

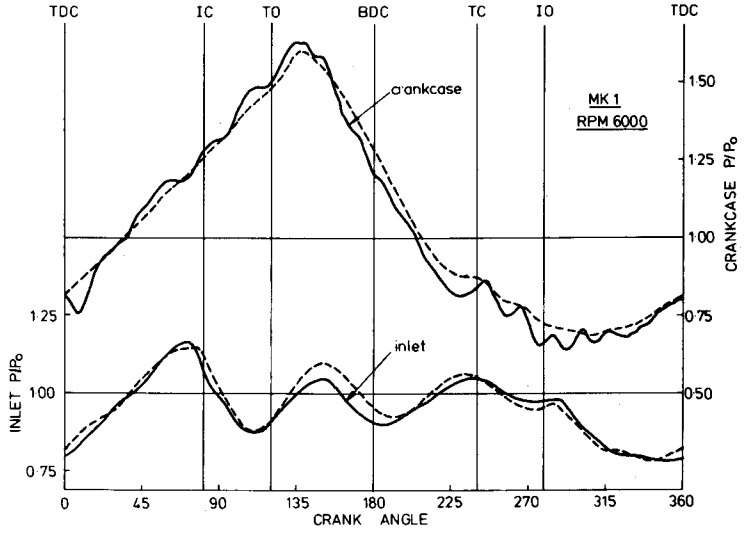

Fig. 21 - Crankcase and inlet pressures for MK1 at 6000 rpm

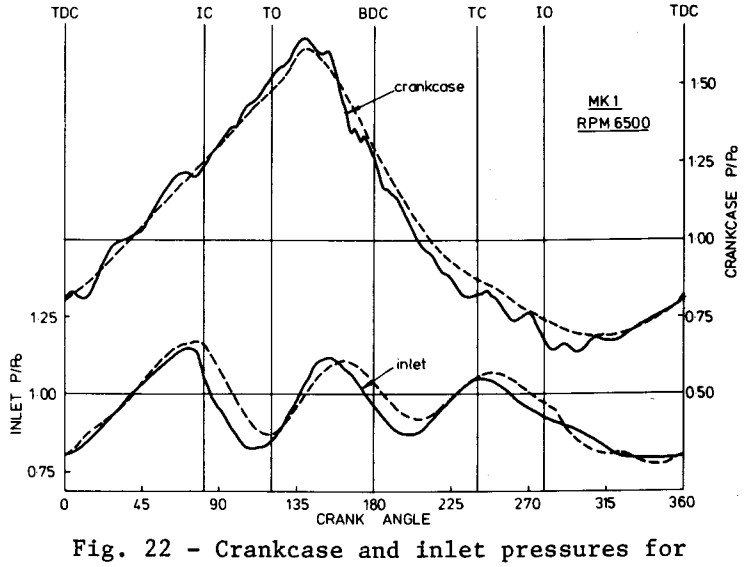

Fig. 22 - Crankcase and inlet pressures for MK1 at 6500 rpm

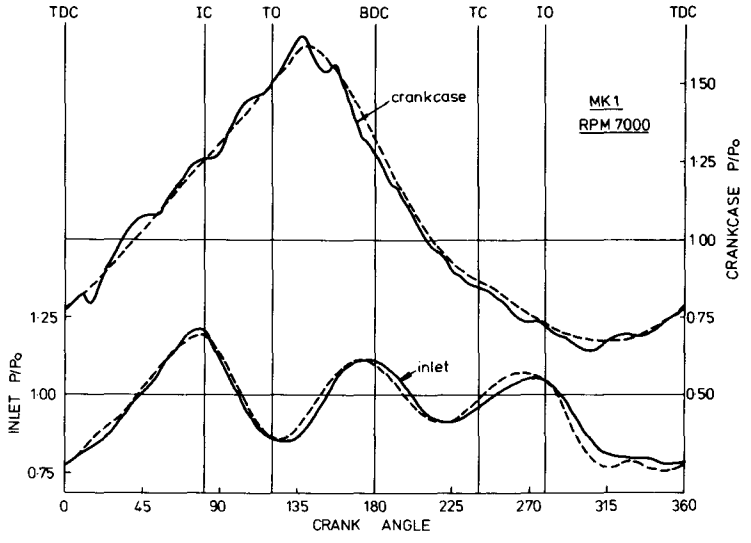

Fig. 23 - Crankcase and inlet pressures for MK1 at 7000 rpm

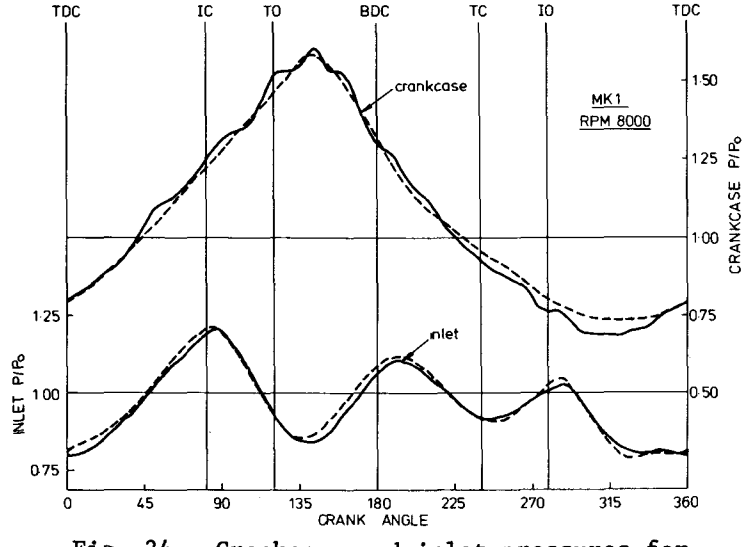

Fig. 24 - Crankcase and inlet pressures for MK1 at 8000 rpm

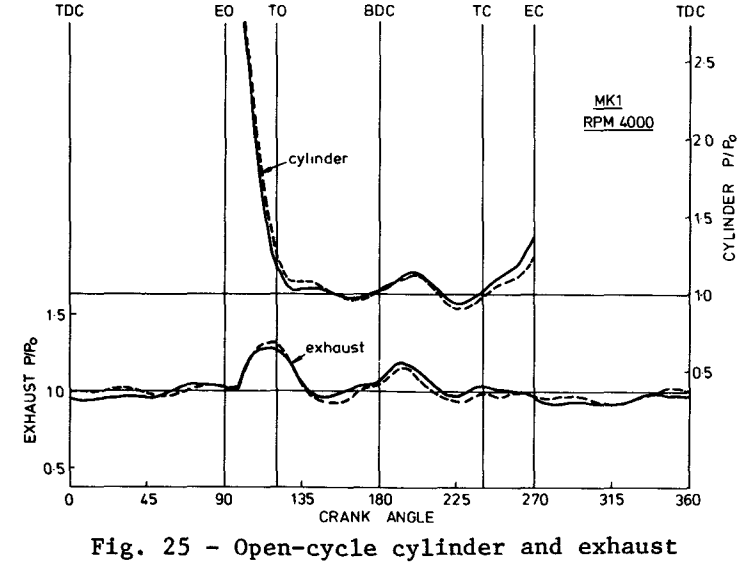

Fig. 25 - Open-cycle cylinder and exhaust pressures of MK1 at 4000 rpm

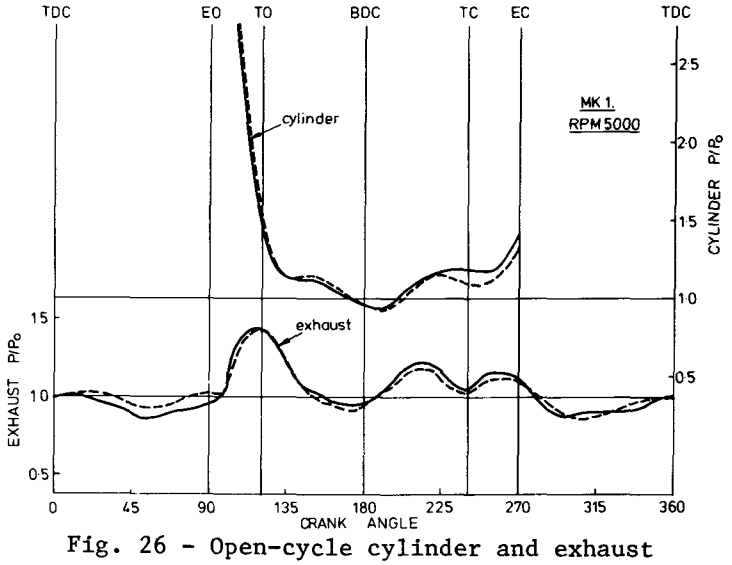

Fig. 26 - Open-cycle cylinder and exhaust pressures of MK1 at 5000 rpm

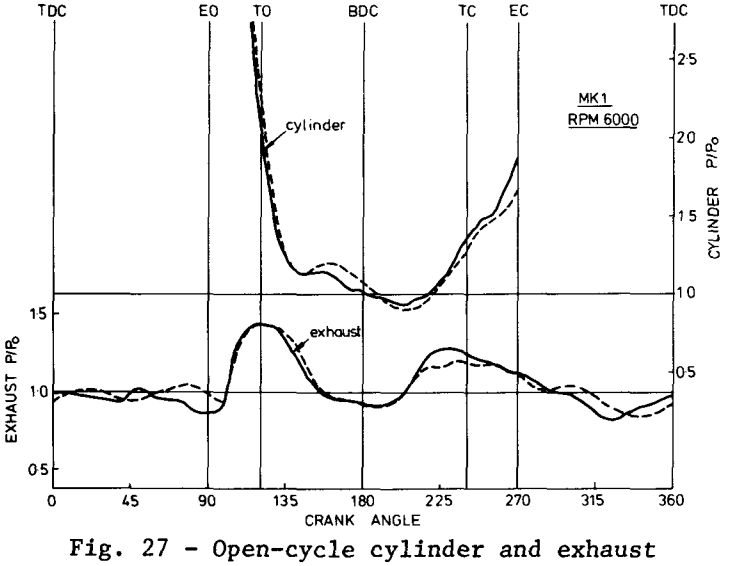

Fig. 27 - Open-cycle cylinder and exhaust pressures of MK1 at 6000 rpm

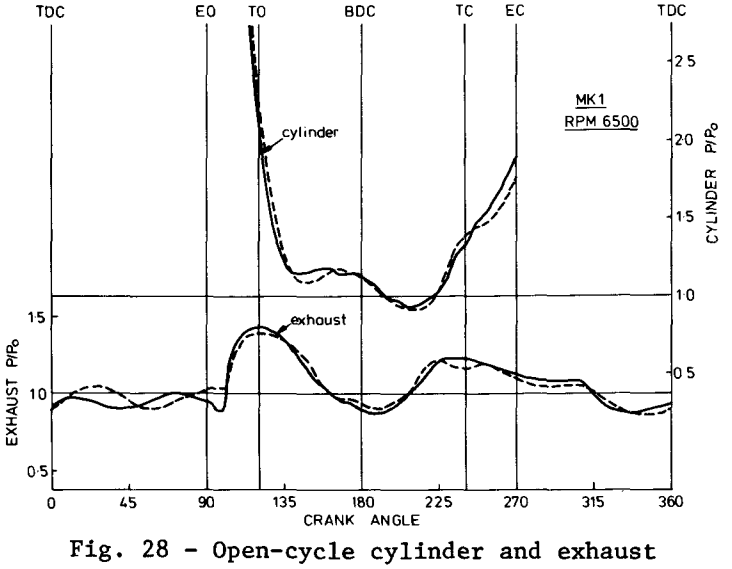

Fig. 28 - Open-cycle cylinder and exhaust pressures of MK1 at 6500 rpm

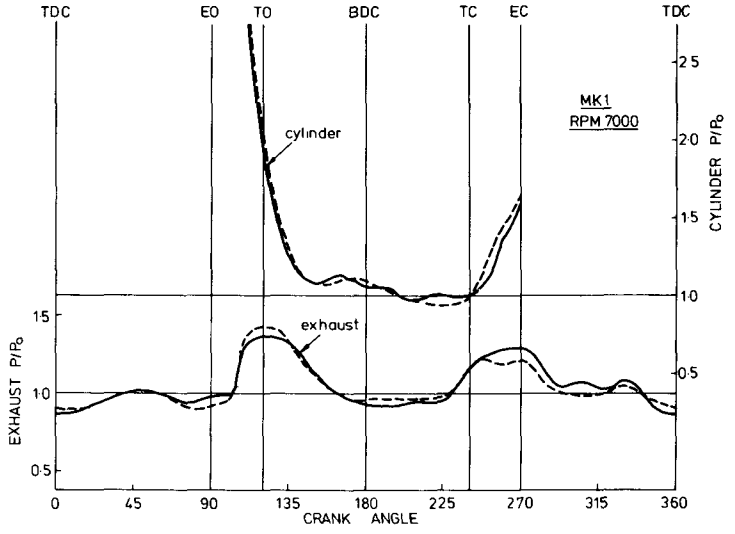

Fig. 29 - Open-cycle cylinder and exhaust pressures of MK1 at 7000 rpm

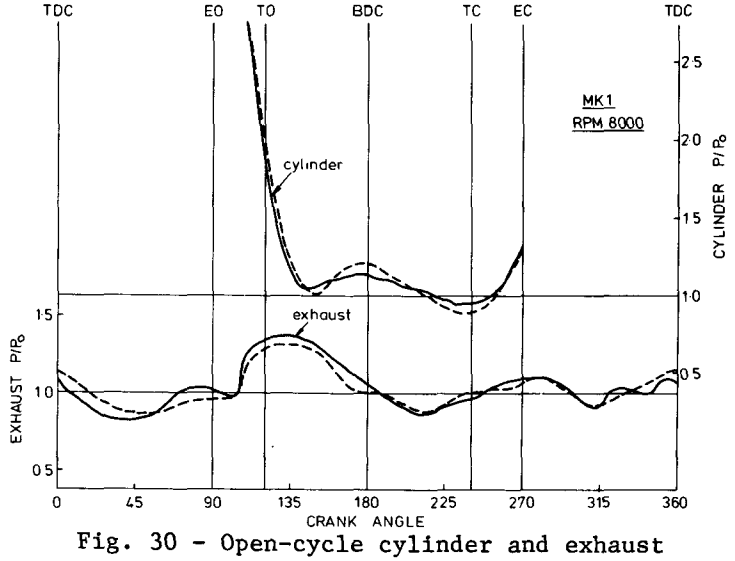

Fig. 30 - Open-cycle cylinder and exhaust pressures of MK1 at 8000 rpm

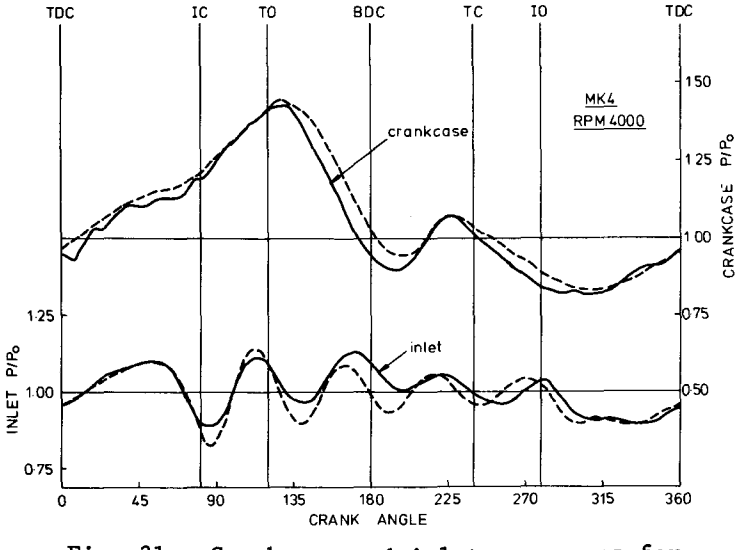

Fig. 31 - Crankcase and inlet pressures for MK4 at 4000 rpm

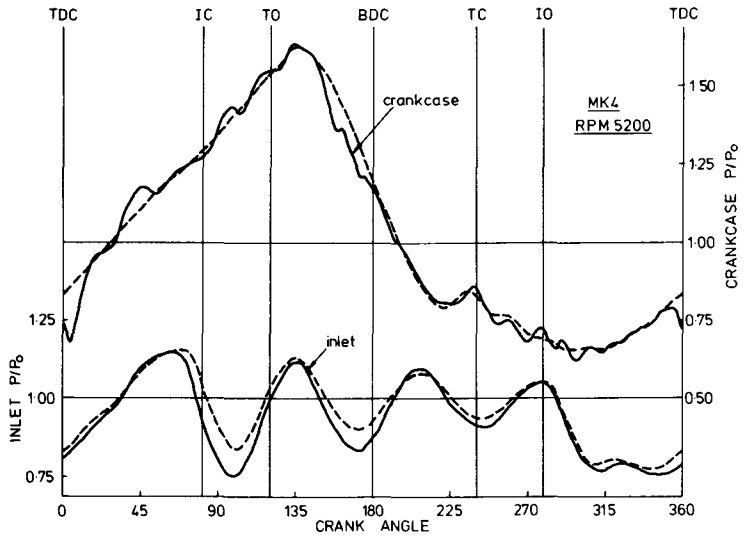

Fig. 32 - Crankcase and inlet pressures for MK4 at 5200 rpm

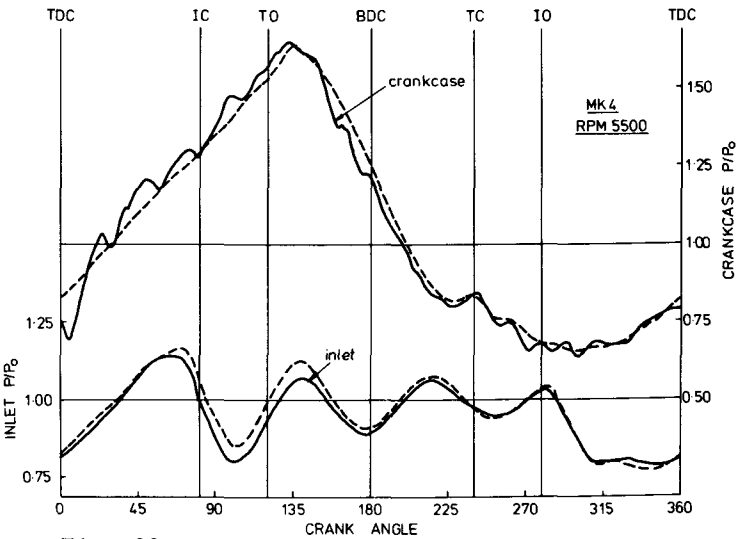

Fig. 33 - Crankcase and inlet pressures for MK4 at 5500 rpm

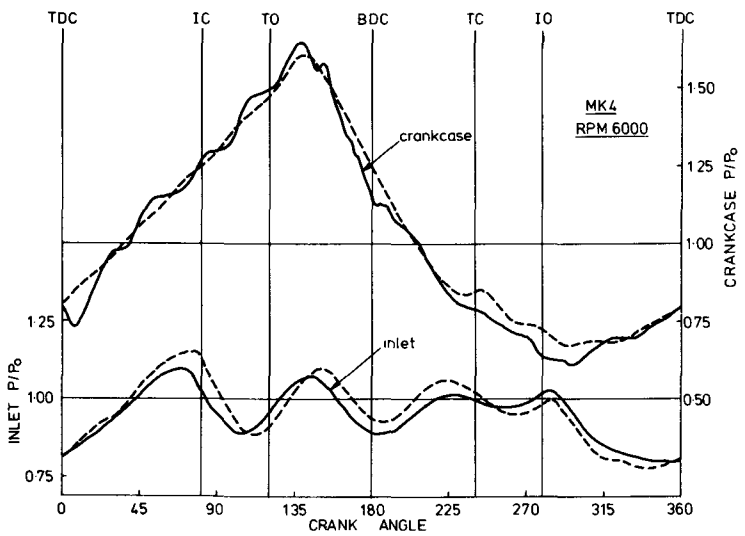

Fig. 34 - Crankcase and inlet pressures for MK4 at 6000 rpm

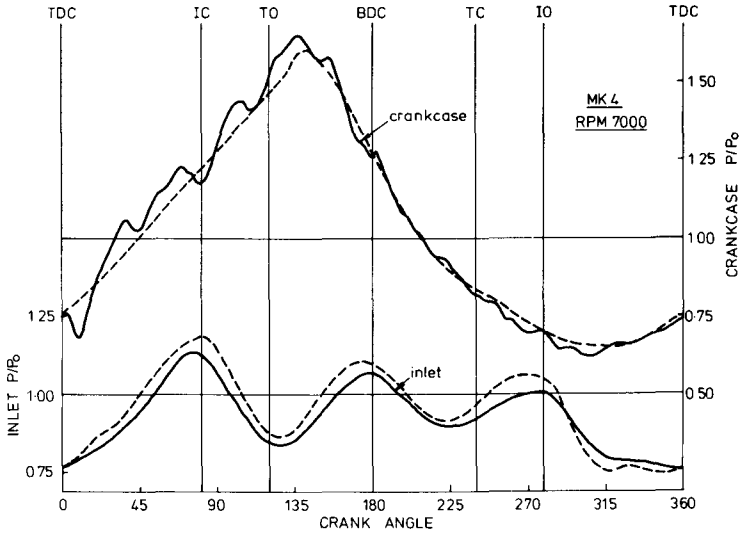

Fig. 35 - Crankcase and inlet pressures for MK4 at 7000 rpm

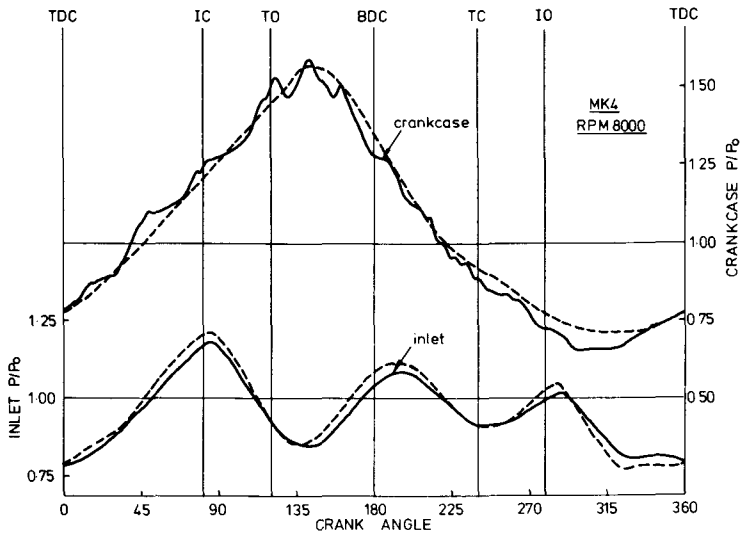

Fig. 36 - Crankcase and inlet pressures for MK4 at 8000 rpm

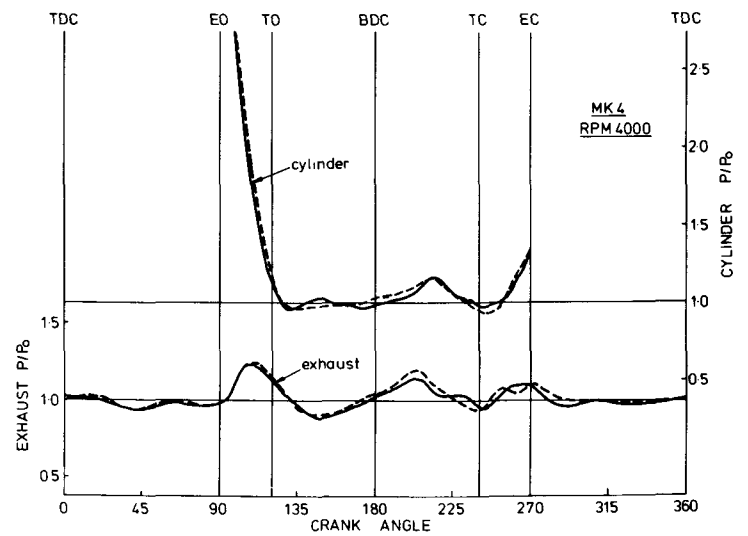

Fig. 37 - Open-cycle cylinder and exhaust pressure of MK4 at 4000 rpm

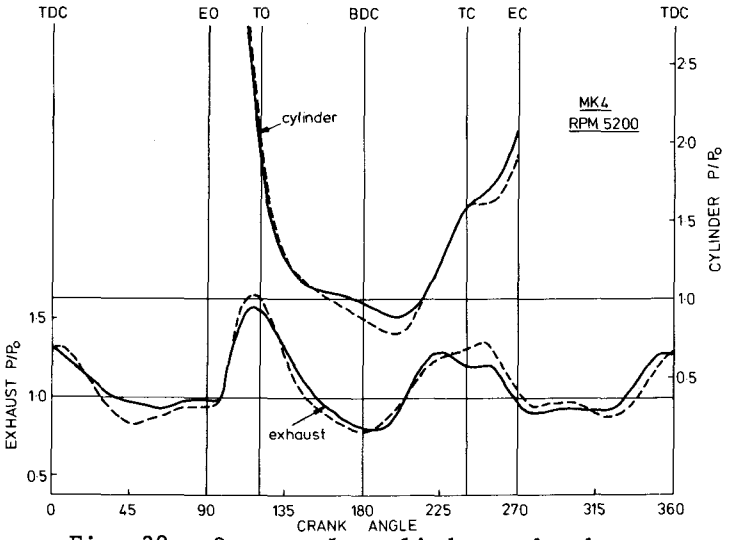

Fig. 38 - Open-cycle cylinder and exhaust pressure of MK4 at 5200 rpm

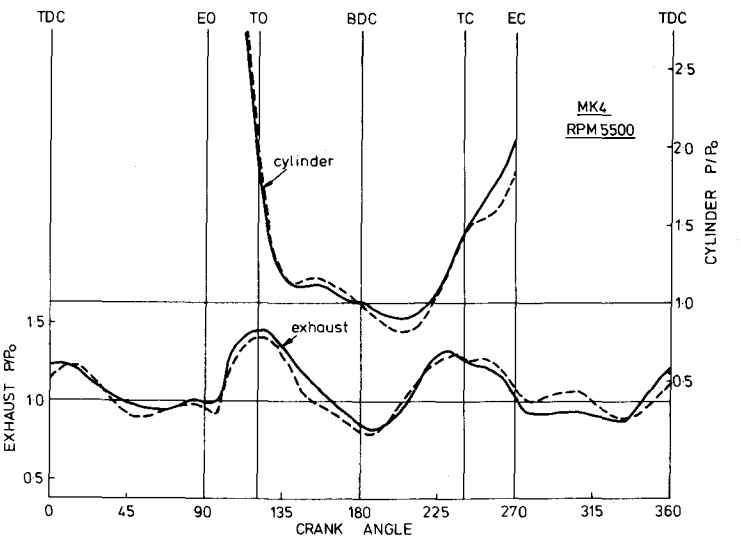

Fig. 39 - Open-cycle cylinder and exhaust pressure of MK4 at 5500 rpm

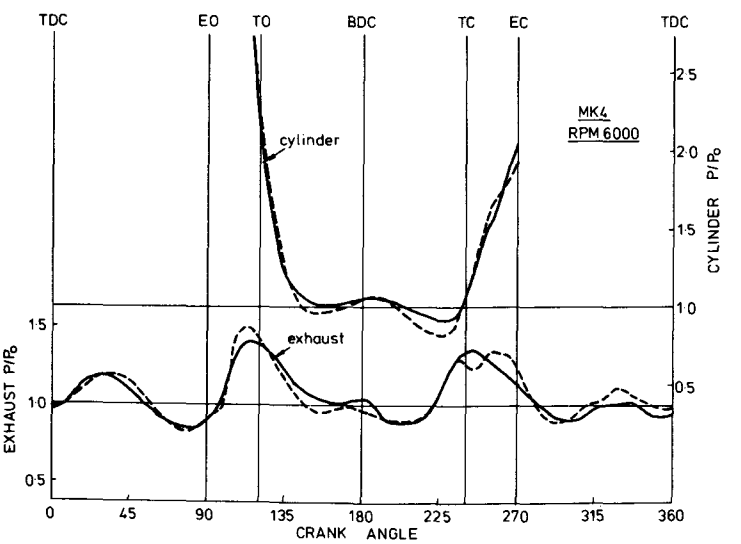

Fig. 40 - Open-cycle cylinder and exhaust pressure of MK4 at 6000 rpm

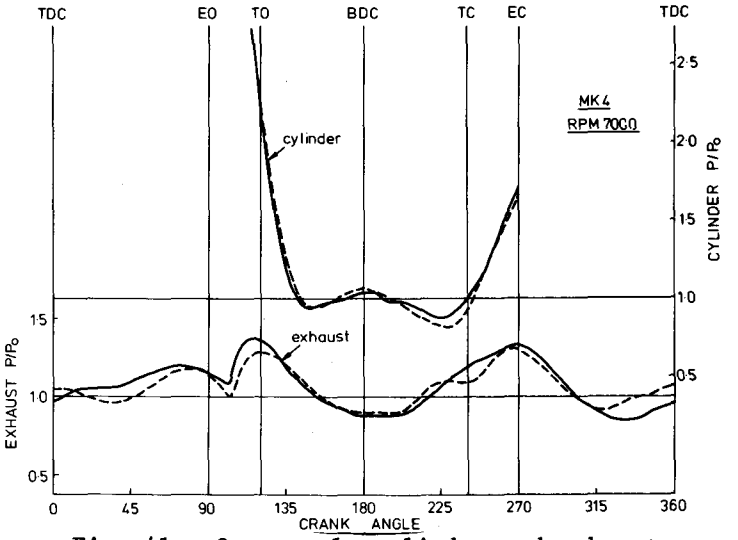

Fig. 41 - Open-cycle cylinder and exhaust pressure of MK4 at 7000 rpm

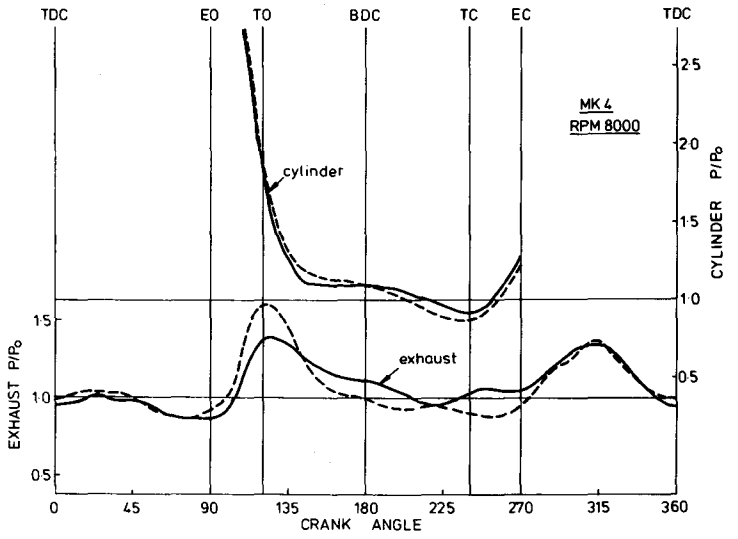

Fig. 42 - Open-cycle cylinder and exhaust pressure of MK4 at 8000 rpm

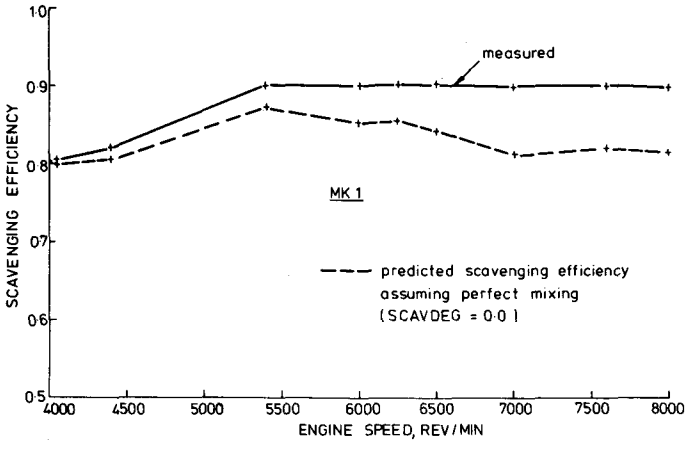

Fig. 43 - Measured and predicted scavenging efficiency for MK1 system

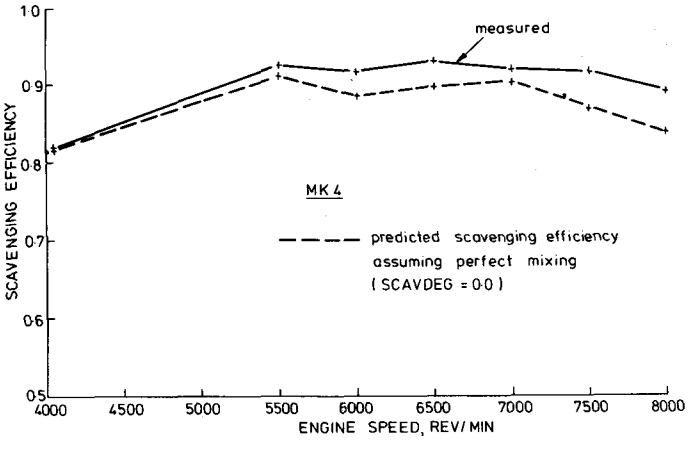

Fig. 44 - Measured and predicted scavenging efficiency for MK4 system

well the scavenge or gas exchange process in the cylinder. However, as the theoretical model is flexible in that the number of crankangle degrees of perfect scavenging, SCAVDEG, is a variable, it is possible to find a value of SCAVDEG which, when inserted into the 'Throughflow' program, gives precise correlation of the theoretical with the measured scavenging efficiency. This is done and Fig. 45 shows for both exhaust systems that

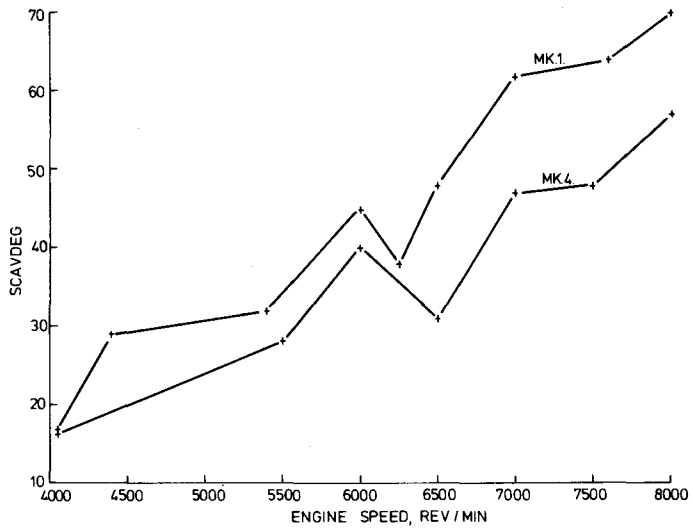

Fig. 45 - Variation of SCAVDEG with engine speed for MK1 and MK4 systems

required value of SCAVDEG at each engine speed to give perfect theory/measurement agreement. It can then be seen that scavenging efficiency is both a speed and flow dependent phenomena, flow dependent in the sense that the MK4 system requires fewer SCAVDEG for correlation for it has a higher delivery ratio than the MK3 system.

As a matter of interest, when this engine was scavenge tested with the Jante approach described by Blair (10), the mean-velocity contour diagram was found to be stable, cohesive, and similar at all engine speeds from 4000 to 8000 rev/min and that "the mean-velocity function, Mean Velocity Ratio, was also linear with respect to engine speed". Naturally, the scavenge process is a partly unsteady gas-dynamics and partly fluid-mechanics phenomenon and the value of SCAVDEG will be related in some fashion to all of the parameters mentioned in the preceding paragraphs.

DELIVERY RATIO AND CHARGING EFFICIENCY

The 'Throughflow' program also predicts the fresh charge, or airflow rate through the engine and a comparison of the measured (full line) and calulated (dashed line) delivery ratios for the MK1 and MK4 exhaust systems is illustrated in Figs. 46 and 47. Measurements and calculations correlate well,

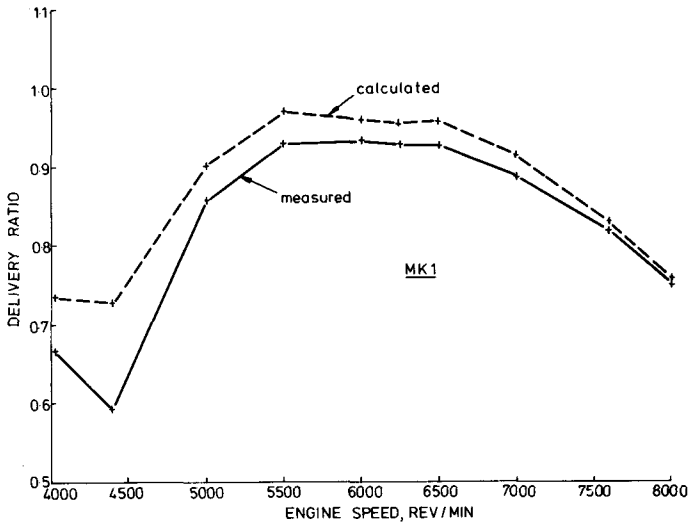

Fig. 46 - Comparison of measured and predicted delivery ratios for MK1 system

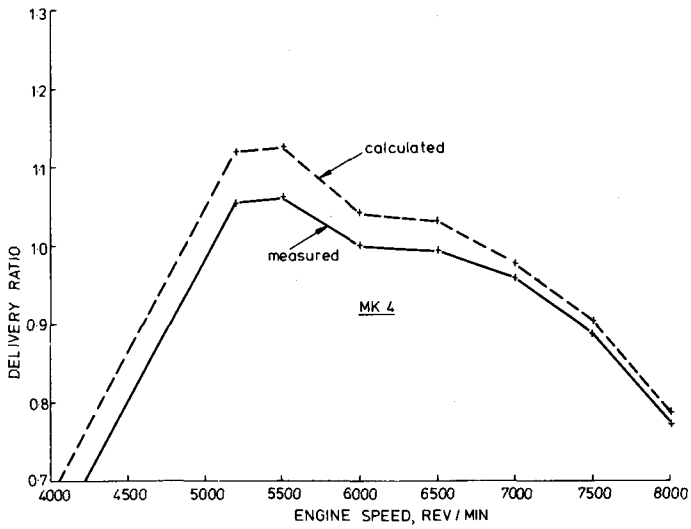

Fig. 47 - Comparison of measured and predicted delivery ratios for MK4 system

both in level and with respect to changing engine speed.

Charging efficiency, calculated as in Eq. 13, is predicted with the Throughflow program, using those values of SCAVDEG illustrated in Fig. 45, that is, for perfect correlation between measured and calculated scavenging efficiencies. The resulting charging efficiencies for the MK'sl and 4 exhaust systems are shown in relation to bmep (full line) with respect to engine speed in Figs. 48 and 49. It is observed that a relationship obviously exists between charging efficiency and torque (or bmep); but what torque would result from a particular and predicted charging efficiency in the case of using the 'Throughflow' program in a design mode would depend in the compression ratio cylinder head shape, ignition type, and several other variables.

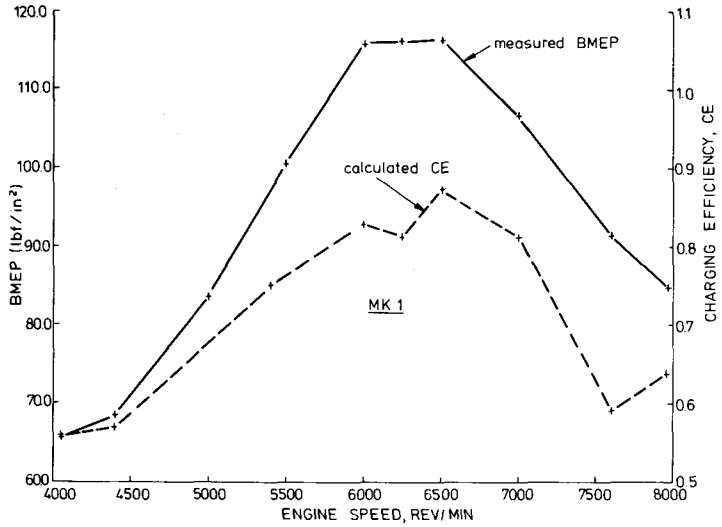

Fig. 48 - Comparison of measured bmep and predicted charging efficiency for MK1 system

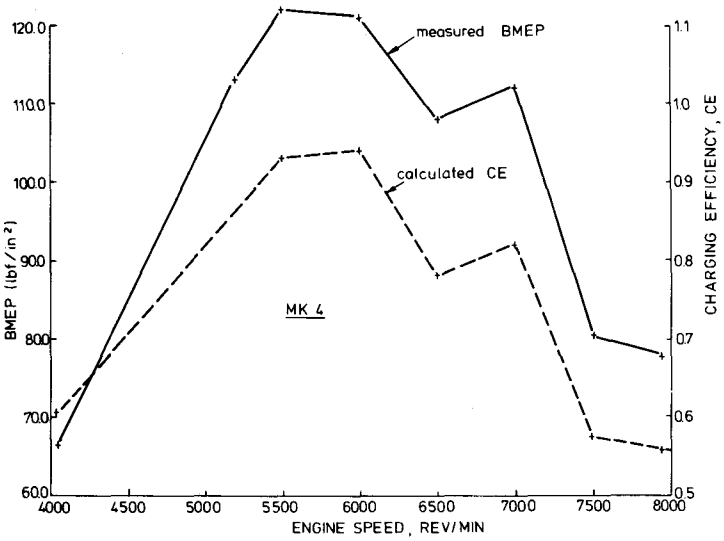

Fig. 49 - Comparison of measured bmep and predicted charging efficiency for MK4 system

CONCLUSIONS

The strong correlation between measurement and calculation for delivery ratio, scavenging efficiency, charging efficiency (bmep), and the exhaust, inlet, crankcase and cylinder pressure diagrams illustrates clearly the ability of the latest version of the 'Throughflow' computer program to predict the unsteady flow through and the gas exchange characteristics of this 250 cm^3 Husqvarna and, by inference, any other small two-cycle unit of similar type. The two-part model for scavenging, denoted by the numeric value of SCAVDEG, proved to be a sound assumption, and it was flexible in that perfect correlation between measurement and calculation could always be obtained and the result of such model manipulation to achieve that effect was a logical relationship between SCAVDEG and the 'fluid-mechanics' of the loop-scavenge process. The final fragment of that last statement is 'not proven' and, currently, efforts are being made at Queen's University to establish a firmer (if any!) relationship between SCAVDEG, Jante scavenging diagrams (10), and measured (or calculated) scavenging efficiency.

Finally, the 'Throughflow' program in its lastest form, predicting accurately as it does the trapped charge total mass and purity, could now be further enhanced in that it becomes worthwhile to attach a combustion or closed cycle model in order to predict torque directly.

NOMENCLATURE

a speed of sound ft/sec.

A	non-dimensional speed of sound a/a_o
AF	air/fuel ratio
bhp	power, hp
bmep	brake mean effective pressure lb/in^2
bsfc	brake specific fuel consumption lb/hp.hr
B	volume fraction of expansion gas remaining in cylinder after scavenging
CM1	cylinder mass at start of time increment, lb
CM2	cylinder mass at end of time increment, lb
Cϕ1	cylinder gas purity at start of time increment
Cϕ2	cylinder gas purity at end of time increment
DR	delivery ratio
EX (1)	purity of gas in first control volume of exhaust pipe
F	area, ft^2
F(N)	area at Nth mesh position, ft^2
L	length, ft
$\dot{m}$	mass rate of flow, lb/sec
M	mass, lb
M1(J)	mass in Jth control volume at start of time increment, lb
M2(J)	mass in Jth control volume at end of time increment, lb
ΔMEX	mass flow from cylinder to exhaust during time increment, lb
ΔMTR	mass flow from transfer to cylinder during time increment, lb
ΔM(N)	mass flow across Nth mesh position during time increment, lb
N	mesh position designation
p	average number of carbon atoms in unburned hydrocarbon molecule
P	pressure, lb/ft^2
q	average number of hydrogen atoms in unburned hydrocarbon molecule
R	gas constant, ft.lbf/lb^oR
S1	moles of oxygen in fresh charge
S2	moles of nitrogen in fresh charge
t	time, sec
T	absolute temperature, ^oR
TRϕ(1)	purity of gas in first control volume of transfer duct
u	particle velocity, ft/sec
U	non-dimensional particle velocity, u/a_o
V	volume, ft^3
VFCOCG	volume fraction of carbon monoxide in compression gas sample
VFCOEG	volume fraction of carbon monoxide in expansion gas sample
VFO2CG	volume fraction of oxygen in compression gas sample
VFO2EG	volume fraction of oxygen in expansion gas sample
W	volume fraction of fresh charge in cylinder after scavenging
X1	moles of carbon monoxide in expansion gas
X2	moles of carbon dioxide in expansion gas
X3	moles of hydrogen in expansion gas
X4	moles of nitrogen in expansion gas
X5	moles of oxygen in expansion gas
X6	moles of hydrocarbon in expansion gas
X7	moles of water in expansion gas
y	effective ratio of hydrogen to carbon atoms in fuel
Z	non-dimensional time, $a_o t/L$
ΔZ	increment of Z
λ,β	Riemann variables, $A \pm (\gamma-1).U/2$
γ	ratio of specific heats
η_c	charging efficiency
η_s	scavenging efficiency
η_T	trapping efficiency
ρ	density, lb/ft^3
ϕ1(J)	purity of gas in Jth control volume at start of time increment
ϕ2(J)	purity of gas in Jth control volume at start of time increment

SUBSCRIPTS

o	reference conditions, usually atmospheric pressure level

ACKNOWLEDGEMENTS

The authors acknowledge their debt to The Queen's University of Belfast and The Department of Mechanical Engineering for the excellent research, computation, workshop and laboratory facilities which has made this work possible; in this regard also the helpful and encouraging attitude of Professor Crossland, Head of Department, over the last decade must also be noted. Financial assistance for the project has been jointly provided by the following: Yamaha Motor-Japan, Husqvarna AB-Sweden, Bombardier Ltd. - Canada, Greeves Motor Cycles - England, McCulloch Corporation - U.S.A., Homelite, Div. Textron - U.S.A., and Mercury Marine - U.S.A. In this connection, further thanks are due to Husqvarna AB for their generous supply of engines and components for the experimental program. A final note of thanks must be extended to all those previous students at Queen's University (7), (8) and (9), without whose computational and experimental building blocks this work could not have been completed.

REFERENCES

1. M. Kadenacy, "Development of the Kadenacy Principle", The Oil Engine, pp 214-217, November 1939.

2. E. Giffen, "Rapid Discharge of Gas from a Vessel into the Atmosphere", Engineering, p 134, August 16, 1940.

3. P. deHaller, "The Application of a Graphic Method to some Dynamic Problems in Gases", Sulzer Tech. Rev. No. 1, p 6, 1945.

4. E. Jenny, "Calculations and Experimental Investigation on Large Amplitude Pressure Waves in the Exhaust Manifold", Doctoral Thesis,

ETH Zurich, 1949.

5. F.J. Wallace and M.H. Nassif, "Air Flow in a Naturally Aspirated Two-Stroke Engine", Proc. I. Mech. E., Vol. 168, p 515, 1954.

6. R.S. Benson, R.D. Garg, and D. Woollatt, "A Numerical Solution of Unsteady Flow Problems", Int. J. Mech. Sci., Vol. 6, p 117, 1964.

7. G.P. Blair and M.B. Johnston, "Unsteady Flow Effects in Exhaust Systems of Naturally Aspirated, Crankcase Compression, Two-Cycle Internal Combustion Engines", SAE Transactions, Vol. 77, 1968, SAE 680594.

8. G.P. Blair and J.A. Arbuckle, "Unsteady Flow in the Induction System of a Reciprocating Internal Combustion Engine", SAE Transactions, Vol. 79, 1970, SAE 700443.

9. G.P. Blair and W.L. Cahoon, "A More Complete Analysis of Unsteady Gas Flow Through a High-Specific-Output Two-Cycle Engine", SAE Transactions, Vol. 81, 1972, SAE 720156.

10. G.P. Blair, "Studing Scavenge Flow in a Two-Stroke Cycle Engine", SAE-FCIM meeting, Milwaukee, September 1975, SAE 750752.

11. T. Asunuma and S. Yanagihara, "Gas Sampling Valve for Measuring Scavenging Efficiency in High-Speed Two-Stroke Engines", SAE Transactions, Vol. 70, p 420, paper T-47, 1962.

12. R.R. Booy, "Evaluating Scavenging Efficiency of Two-Cycle Gasoline Engines", SAE paper 670029, 1967.